



## Leaching efficiency and kinetics of the recovery of palladium and rhodium from a spent auto-catalyst in HCl/CuCl<sub>2</sub> media

Carlos A. Nogueira, Ana Paula Paiva, Maria Clara Costa & Ana M. Rosa da Costa

To cite this article: Carlos A. Nogueira, Ana Paula Paiva, Maria Clara Costa & Ana M. Rosa da Costa (2019): Leaching efficiency and kinetics of the recovery of palladium and rhodium from a spent auto-catalyst in HCl/CuCl<sub>2</sub> media, Environmental Technology, DOI: [10.1080/09593330.2018.1563635](https://doi.org/10.1080/09593330.2018.1563635)

To link to this article: <https://doi.org/10.1080/09593330.2018.1563635>



Published online: 03 Jan 2019.



Submit your article to this journal [↗](#)



Article views: 32



View Crossmark data [↗](#)



## Leaching efficiency and kinetics of the recovery of palladium and rhodium from a spent auto-catalyst in HCl/CuCl<sub>2</sub> media

Carlos A. Nogueira<sup>a</sup>, Ana Paula Paiva<sup>b</sup>, Maria Clara Costa<sup>c</sup> and Ana M. Rosa da Costa<sup>d</sup>

<sup>a</sup>Laboratório Nacional de Energia e Geologia, I.P., Lisboa, Portugal; <sup>b</sup>Faculdade de Ciências, Centro de Química e Bioquímica / Centro de Química Estrutural, Universidade de Lisboa, Lisboa, Portugal; <sup>c</sup>Faculdade de Ciências e Tecnologia, Departamento de Química e Farmácia, Centro de Ciências do Mar, Universidade do Algarve, Faro, Portugal; <sup>d</sup>Faculdade de Ciências e Tecnologia, Departamento de Química e Farmácia, Centro de Investigação em Química do Algarve, Universidade do Algarve, Faro, Portugal

### ABSTRACT

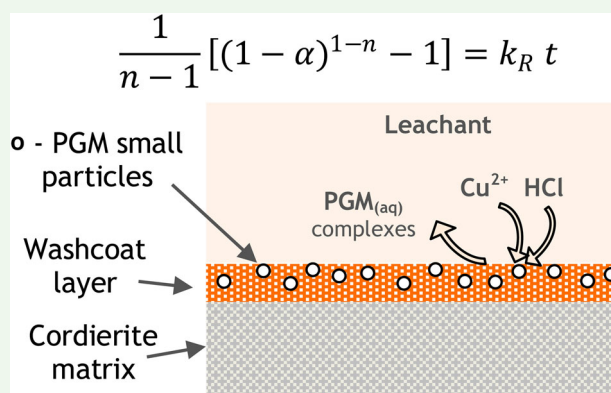
The recycling of scarce elements such as platinum-group metals is becoming crucial due to their growing importance in current and emerging applications. In this sense, the recovery of palladium and rhodium from a spent auto-catalyst by leaching in HCl/CuCl<sub>2</sub> media was studied, aiming at assessing the kinetic performance as well as the influence of some processing factors, and the behaviour of contaminant metals. Based on a kinetic model developed for the present case, the influence of temperature was evaluated and the corresponding values of activation energy were estimated as  $60.1 \pm 4.1 \text{ kJ mol}^{-1}$  for Pd and  $44.3 \pm 7.3 \text{ kJ mol}^{-1}$  for Rh, indicating the relevance of the chemical step rather than diffusion. This finding was corroborated by the non-significant influence of the stirring velocity. The reaction orders were estimated for each leaching reagent: for HCl, values of  $2.1 \pm 0.1$  for Pd and  $1.0 \pm 0.3$  for Rh were obtained; for Cu<sup>2+</sup>, the obtained values were  $0.42 \pm 0.04$  for Pd and  $0.36 \pm 0.06$  for Rh. Without any significant loss of efficiency, solutions with higher metal concentrations were obtained using lower liquid/solid ratios, such as 5 L/kg. The main contaminant in solution was aluminum, and its leaching was found to be very dependent on the temperature and acid concentration.

### ARTICLE HISTORY

Received 24 September 2018  
Accepted 19 December 2018

### KEYWORDS

Leaching; Pd-Rh catalyst; Hydrometallurgy; kinetics; recycling



### Introduction

Recycling of platinum-group metals (PGMs) from waste materials, namely from catalytic converters, is gaining growing importance due to the scarcity, economic importance and criticality of those noble metals [1–3]. Moreover, spent catalysts are hazardous wastes that should be correctly managed in order to avoid environmental damage. Recycling is therefore mandatory for both economic and environmental reasons.

Although pyrometallurgical processing has been commonly used in industrial practice [4,5], direct hydrometallurgical treatment of catalysts is an option that has

been pursued. Several hydrometallurgical routes have been proposed and reviewed [6,7]; usually they are based on a leaching step in hydrochloric acid media, involving different oxidants, such as hydrogen peroxide [8–10], nitric acid [8,11–14] and sodium hypochlorite [15]. The spent catalysts can be pretreated by heating under different atmospheres before the leaching step, as proposed in some works [16]. Alternative methods were also considered, such as salt roasting followed by water or HCl leaching [17,18], or even microwave-assisted HCl leaching [19]. After the leaching step, several options can be considered for recovering the

PGMs from the leachates, such as solvent extraction, cementation and selective precipitation. The recovery of some secondary metals co-dissolved, such as aluminum and cerium, is also an issue that has been considered, as well as the possibility of recycling the spent acidic chloride liquors to the leaching operation [20].

The present authors proposed a new process for the leaching of a Pd-Rh catalyst using the mixture HCl/CuCl<sub>2</sub> as leaching medium [21]. In this process the cupric ion was used as oxidizing agent, promoting the dissolution of the PGMs as chlorocomplexes. The several factors affecting the leaching were then studied and optimized through a factorial design methodology, in order to evaluate the effects of temperature, time, and HCl and Cu<sup>2+</sup> concentrations. Some aspects regarding this leaching medium were nevertheless not fully investigated at that time. One of them is the kinetics of the leaching reaction. The evaluation of the reaction rates is very important to better understand how the system behaves, allowing the development of tools for reactor and process design. Another aspect requiring investigation is the behaviour shown by the other metals present in the spent catalyst in those leaching media. Therefore, this paper describes the results of the leaching studies of a spent Pd-Rh auto-catalyst in HCl/CuCl<sub>2</sub> media, regarding the above mentioned features.

## Materials and methods

The raw material used in this work is a spent Pd-Rh catalyst in ceramic substrate (with cordierite-based honeycomb monolith morphology). The catalyst was grinded using a cutting mill (IKA MF10) with a 3 mm discharge grid. The material so obtained (called standard) was used in the majority of the leaching lab work. Other procedures were adopted for the tests aiming to evaluate the effect of the particle size: for producing a fine material sample, a disk mill (N.V. Tema) was utilized; for the coarse material, a slice of monolith was gently grinded by a hand mortar. The grinded materials were sampled using a rotating divider (spinning riffler Microscal). Depending on the size range, the particle size distribution was assessed by two techniques: for the fine material, a laser diffraction granulometer (CILAS 1064) was utilized, while for the standard and coarse materials the sieving technique was adopted, with adequate sieve series apparatus (Retsch AS-200 vibrating shaker). The average particle sizes  $d_{50}$  obtained for the coarse, standard and fine samples were 1.0, 0.61 and 0.016 mm, respectively. The Pd and Rh concentrations in the spent catalyst were in the ranges 420–470 mg kg<sup>-1</sup> and 220–290 mg kg<sup>-1</sup>, respectively.

The leaching experiments were conducted in 200 mL glass cylindrical vessels, equipped with mechanical stirring (with a 2-blade impeller) and temperature control system. The stirring velocity was constant in most of the tests ( $sv = 250 \text{ min}^{-1}$ ) except when this factor was the object of study. Most of the experimental leaching tests were performed at constant values of liquid/solid ratio ( $R_{L/S} = 20 \text{ L kg}^{-1}$ ) unless when this factor was specifically evaluated. The counting of the reaction time began when the solids were added to the reactor containing the leachant mixture, at the set temperature of each test. Small aliquots were taken at several times, the collected samples were centrifuged and the solutions sent for metal analysis. At the end of the experiment the leachates were filtered. To verify the mass balances, the solid residues were washed and dried, in order to evaluate the involved weight losses.

The final free acidity of the leachates was determined by titration with standard 1.0 M NaOH solution, using methyl orange as indicator. Since the colour change of the indicator occurs at relatively low pH, any precipitation during the test is prevented.

The analysis of the metals (Pd, Rh and the accompanying elements Al, Fe, Zn, Ni, Cr, Ca, Ce, La, Zr) was performed by ICP-AES (Horiba Jobin-Yvon Ultima). For the initial solid materials, a digestion in microwave with an acid mixture (HCl/HNO<sub>3</sub>/HF) was accomplished prior to the chemical analysis.

The leaching yields of the metals under study were calculated from the respective concentrations determined in solution, referred to the initial average content in the catalyst sample, pondering with the respective volumes and weights used in each test. In the kinetic studies described in this work, the conversion (of the solid particles of PGMs) is currently utilized instead of the metal yields. However, considering that the only source of metals in solution are the PGMs particles, and that all oxidized atoms are dissolved, the metal leaching yields are equal to the particles conversions, the only difference being the scale used (0%–100% for yields and 0–1 for conversions).

## Results and discussion

### Kinetics of Pd and Rh leaching

The leaching process under study is typically a non-catalytic heterogeneous solid/liquid reaction, whose kinetics is documented in the specialized literature [22–24]. The rate of these reactions can be expressed by the number of moles reacted or formed with time, per unit area of surface where the reaction takes place. For the general reaction of a solid *B* reacting with one or more

leaching agents in solution (e.g.  $A$ ,  $E$ , ...) the rate can be expressed by equation (1),

$$v = -\frac{1}{bA_g} \left( \frac{dN_B}{dt} \right) \quad (1)$$

where  $v$  is the reaction rate,  $b$  a stoichiometric parameter,  $A_g$  the reacting area of the grain surface,  $N_B$  the number of moles of the solid phase and  $t$  the time. By transforming the previous equation into a form allowing the experimental control of the reaction progress, namely by using the conversion  $\alpha$ , related with the number of moles of the reacting solid as  $N_B = N_{B0} (1 - \alpha)$  (where the subscript 0 refers to the initial conditions) the expression depicted in equation (2) can be obtained,

$$v = \frac{N_{B0}}{bA_g} \left( \frac{d\alpha}{dt} \right) = \frac{V_{B0}\rho}{bA_g} \left( \frac{d\alpha}{dt} \right) \quad (2)$$

where  $\rho$  and  $V_B$  represent the molar density and the volume of the solid particle, respectively. The reaction rate is also proportional to the concentration ( $C$ ) of the involved intervenient phases and reactants, through the rate constant,  $k$ , according to the law of mass action, equation (3),

$$v = k C_A^a C_E^e C_B^n \quad (3)$$

where  $A$  and  $E$  refer to the leachant reagents (e.g. an acid like HCl and an oxidant like  $\text{Cu}^{2+}$ ) and  $B$  to the solid (the PGMs). The parameters  $a$ ,  $e$  and  $n$  are the power factors reflecting the effect of the involved concentrations on the reaction rates, usually called the reaction orders.

In heterogeneous reactions, the concentrations of substances in solution are the only ones typically considered in this formulation. However, a more general approach is followed in this paper, where also the solid phase concentration of  $B$  species,  $C_B$ , is pondered, either expressed in moles per unit volume of the solid or as mole fraction, or by another adequate form. This methodology allows expressing the concentration of  $B$  in the solid as a function of its conversion,  $C_B = C_{B0} (1 - \alpha)$ , which will be helpful to obtain the final rate equation in a measurable form. The other concentrations (of  $A$  and  $E$ ) could also be expressed taking the conversion into account, but a simplification can be made to allow an easier mathematic manipulation of the rate equations. Hence, provided there is an excess of reagents  $A$  and  $E$ , their concentration can be considered constant (or with negligible variation) and therefore only the reacting solid particles are expressed as a function of the conversion. This is valid for the present case, since the consumption of the reagents due to the PGMs leaching is negligible; accordingly, even considering that other metals can be leached, such as aluminum, the

quantities reacted are still not substantial regarding the total acid concentration (this fact will be deeply analyzed later in the Results section, when discussing the leaching behaviour of aluminum). Furthermore, even when aluminum dissolution is more extensive (e.g. at higher temperatures and HCl concentrations) it dissolves slowly (as it will also be seen later), and so in the time region where PGMs kinetics is being evaluated the reagents variation is negligible. Based on the previous assumptions, when expressing in equation (3) the relation between  $C_B$  and conversion, and applying it in equation (2), the differential rate equation depicted in equation (4) is obtained,

$$\left( \frac{d\alpha}{dt} \right) = \frac{b A_g C_A^a C_E^e C_{B0}^n}{V_{B0}\rho} k (1 - \alpha)^n = k_R (1 - \alpha)^n \quad (4)$$

where  $k_R$  represents an apparent rate constant incorporating all the parameters not changing with time, valid for a specific set of experimental conditions, equation (5),

$$k_R = \frac{b A_g C_A^a C_E^e C_{B0}^n}{V_{B0}\rho} k \quad (5)$$

and depending on the temperature ( $T$ ) in the same way as the real kinetic constant, given by the Arrhenius relation, equation (6),

$$k_R = k_0 \exp\left(-\frac{E_A}{RT}\right) \text{ or } \ln k_R = \ln k_0 - \frac{E_A}{RT} \quad (6)$$

where  $E_A$  is the activation energy,  $k_0$  a proportionality constant, and  $R$  the gas constant.

The integration of equation (4) leads to the final integrated rate equation that can be applied to the experimental data, as presented in equation (7).

$$\frac{1}{n-1} [(1-\alpha)^{1-n} - 1] = k_R t, \quad n \neq 1 \quad (7)$$

The first member of equation (7) is a function called  $g(\alpha)$ . This expression is the general rate equation adopted in this work, instead of the expressions normally used, based on geometrical models such as the shrinking core or the shrinking particle models [22–24]. In fact, an evaluation of the reaction characteristics led us to decline the use of these classical models, since their assumptions – a particle with a set geometry that shrinks with time until it completely dissolves – is not observed in the present case. As documented in the literature [25], the spent catalyst processed in this work is a honeycomb structure of ceramic (cordierite) matrix with a thin layer of alumina in its exterior surface (washcoat), where the particles of the PGMs are distributed (Figure 1). The cordierite does not react with the leach medium, hence the particles size and shape do not change significantly during the reaction. Even considering that the washcoat

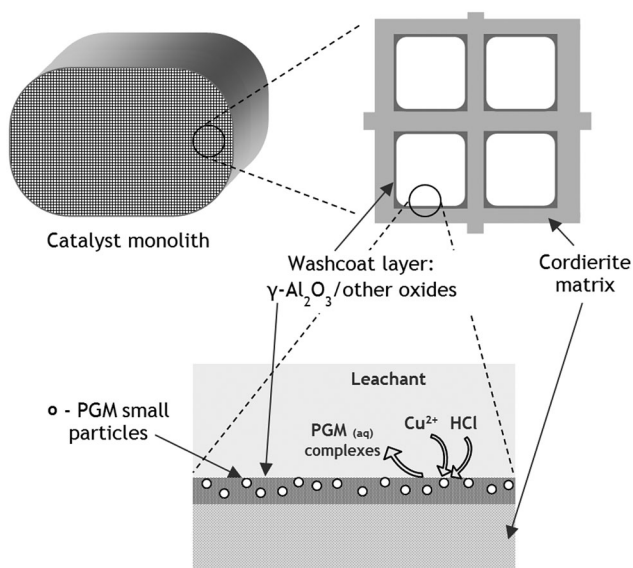


**Figure 1.** Scheme describing the solid composition of the spent catalyst and the reaction of PGMs particles with the leaching agents.

layer can react and dissolve (at least partially), this is only a small part of the total weight of the solid particles. Accordingly, any model dealing with particle shrinking phenomena seems inadequate. It is worth mentioning that attempts to apply these models to the experimental data were nevertheless made, but poor results were indeed obtained.

### Influence of temperature

The influence of temperature on Pd and Rh recoveries along the reaction time was evaluated in a series of experimental tests, carried out at several temperatures. The remaining conditions were maintained constant. As shown in Figure 2, the variation of temperature has a pronounced effect, mainly at the initial times, which

**Table 1.** Values of coefficient  $n$  on equation (7) and apparent rate constants for different temperatures ( $[\text{HCl}] = 2 \text{ M}$ ;  $[\text{Cu}^{2+}] = 0.05 \text{ M}$ ).

Temperature (°C)	Pd			Rh		
	$n_i$	$n$	$k_R \text{ (h}^{-1}\text{)}$	$n_i$	$n$	$k_R \text{ (h}^{-1}\text{)}$
25	1.6	1.6	0.237	6.8	6.7	0.125
40	4.2	4.18	3.04	6.6	6.7	0.663
60	4.3	4.18	9.45	5.2	4.9	0.984
80	3.7	4.18	46.4	4.9	4.9	1.65
100	4.5	4.18	111	4.6	4.9	7.87

is attenuated as the reaction proceeds. The reactions are really faster at higher temperatures, where the metal yields observed at 5 min are close to the maximum achievable. Pd yields are clearly higher than those of Rh. At 100°C, yields close to 83% for Pd and 66% for Rh were reached after 2 h.

The application of the integrated rate expression – equation (7) – to the experimental data requires the knowledge of parameter  $n$ . The determination of this parameter was made as described in sequence. Firstly, the data  $(\alpha, t)$  for each test was adjusted according to the linear relation  $g(\alpha) = k_R t$  (the origin of the straight line being zero) through the variation of the  $n$  values, and the best fit achieved by the squared correlation coefficient was then evaluated. For each case, the value of  $n$  allowing the best fit was subsequently found, being called  $n_i$  (see Table 1). As can be seen for Pd, most of the values determined were not quite different, except for the lowest temperature (25°C). For the range 40°C–100°C an average value of  $n$  can be adopted ( $4.18 \pm 0.34$ ), while for 25°C the value of  $n$  is different (1.6). This difference clearly shows a change in the reaction mechanism for the lowest temperature. For Rh two distinct regions were also found; however, the differences between  $n_i$  values were not so evident as for Pd. Average  $n$  values of  $6.7 \pm 0.2$  and  $4.9 \pm 0.3$  for 25°C–40°C and 60°C–100°C, respectively, were considered.

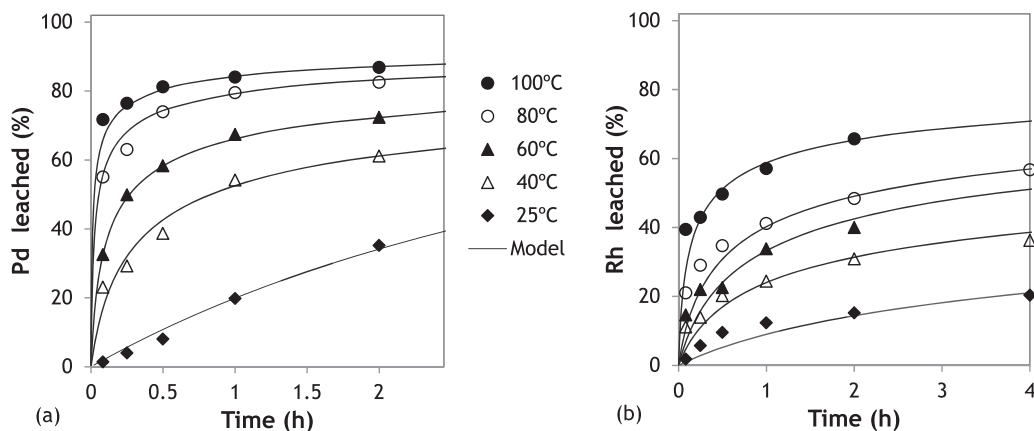


**Figure 2.** Experimental and theoretical leaching yields obtained at different temperatures, for (a) Pd, and (b) Rh ( $[\text{HCl}] = 2 \text{ M}$ ;  $[\text{Cu}^{2+}] = 0.05 \text{ M}$ );  $R_{L/S} = 20 \text{ L kg}^{-1}$ ;  $d_{50} = 0.61 \text{ mm}$ ;  $sv = 250 \text{ min}^{-1}$ ).

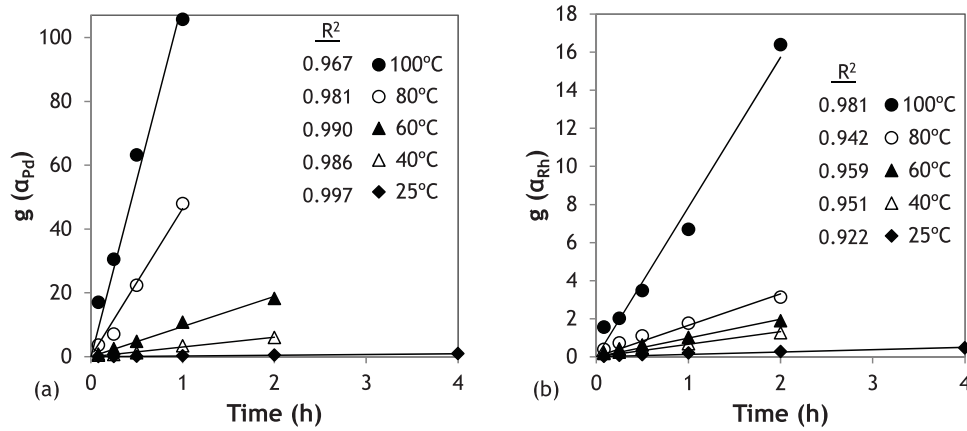


**Figure 3.** Application of the integrated rate equation to the experimental data acquired at different temperatures, for (a) Pd, and (b) Rh.

The application of the integrated rate expression to the experimental data for the adopted values of  $n$  is depicted in Figure 3. Note that the experimental values considered in the application of the model were only those before the stabilization of the leaching yields (for reaction times before that occurrence), to avoid strong deviations. It can generally be said that the experimental data fit reasonably to the linear relation, with some deviations in a few points, which can be explained by the occurrence of experimental errors. These deviations essentially affect the first points (e.g. for 5 min), where less accuracy due to lack of mixture, temperature gradients and sampling errors can be expected (e.g. the time elapsed between the sampling and the separation of the liquid from the solid). The slopes of the linear fits are the apparent rate constants, presented in Table 1. The curves of leaching yields *versus* time, predicted from the model and expressed by equation (7), were therefore determined and are plotted in Figure 2, together with the experimental data, where it is seen that they are a good estimation of the reaction progress at the different temperatures.

Figure 4 shows the result of the application of the Arrhenius plot – equation (6) – using the obtained rate constants. For Pd, two different regions were identified: one in the range 40°C–100°C and the other between

25°C and 40°C. This behaviour is attributed to the different contributions of diffusion and surface chemical phenomena. At higher temperatures, the chemical reaction is faster and then the diffusion constraints can affect the overall reaction rate; accordingly, the slope of the Arrhenius plot is smaller under these circumstances. Regarding Rh, it is not so easy to assign different behaviours to the diverse ranges of the plot due to the higher fluctuation of the data. Thus, a single straight line was adopted for this case. The activation energies for both metals were estimated as  $60.1 \pm 4.1 \text{ kJ mol}^{-1}$  for Pd and  $44.3 \pm 7.3 \text{ kJ mol}^{-1}$  for Rh. Both are sufficiently expressive to attribute the rate limiting step to the surface chemical reaction, but not high enough to disregard some contributions from the diffusion phenomena at higher temperatures (although clearly less important than the chemical step).

Other authors have also applied kinetic models to PGMs leaching in chloride media. A power rate law was applied to the *aqua-regia* leaching of Pt from a reforming

**Table 2.** Values of coefficient  $n$  on equation (7) and apparent rate constants for different leachants concentrations (temperature = 60°C).

[Cu <sup>2+</sup> ] (M)	[HCl] (M)	Pd			Rh		
		$n_i$	$n$	$k_R$ (h <sup>-1</sup> )	$n_i$	$n$	$k_R$ (h <sup>-1</sup> )
0.05	1	2.8	2.8	2.38	3.0	3.0	0.204
		4.3	4.3	10.6	5.2	5.37	0.850
	4	4.1	4.3	52.2	5.7	5.37	1.00
		6	4.5	4.3	88.0	5.2	5.37
0.01	2	4.1	4.21	4.17	6.0	5.68	0.389
0.05		4.3	4.21	9.79	5.2	5.68	0.929
0.15	4.3	4.15	4.21	13.3	6.0	5.68	1.10
0.30		4.3	4.21	18.2	5.5	5.68	1.39

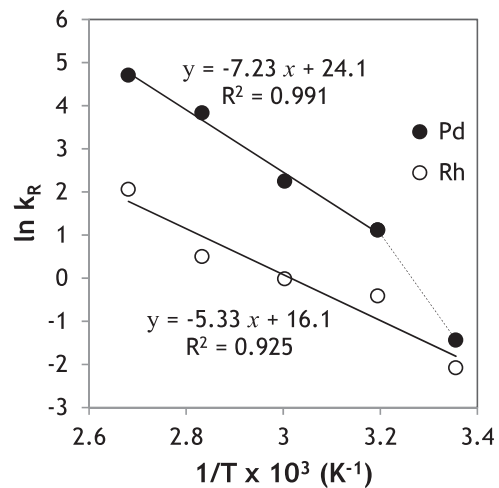


**Figure 4.** Application of the Arrhenius plot to the experimental data, for estimation of the activation energies.

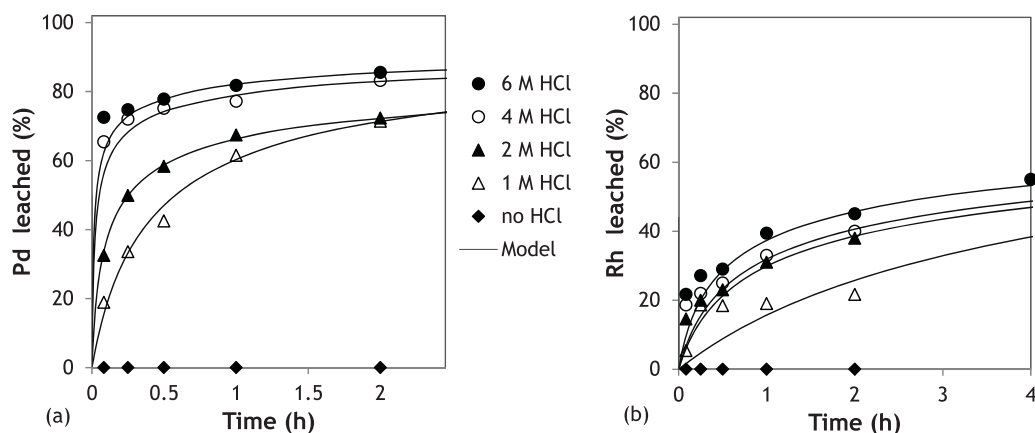


**Figure 5.** Experimental and theoretical leaching yields obtained at different HCl concentrations, for (a) Pd, and (b) Rh ( $60^{\circ}\text{C}$ ;  $[\text{Cu}^{2+}] = 0.05 \text{ M}$ ;  $R_{L/S} = 20 \text{ L kg}^{-1}$ ;  $d_{50} = 0.61 \text{ mm}$ ;  $sv = 250 \text{ min}^{-1}$ ).

catalyst and an activation energy of  $72.1 \text{ kJ mol}^{-1}$  was obtained [26]. The leaching of Pd and Rh from an autocatalyst with  $\text{HCl}/\text{H}_2\text{O}_2/\text{NaClO}$  was also studied, using the unreacted shrinking core model, and values of activation energy of  $63.5$  and  $77.9 \text{ kJ mol}^{-1}$  were found for Pd and Rh, respectively [10].

### Influence of leachants concentration

The influence of the leachants concentration was evaluated by a series of tests where these factors were changed, maintaining the remaining parameters constant. The temperature was set at an intermediate value ( $60^{\circ}\text{C}$ ). For testing the effect of the HCl concentration,  $[\text{Cu}^{2+}]$  was maintained at  $0.05 \text{ M}$ , while for studying the effect of the cupric ion concentration the acid was set at  $2 \text{ M}$ .

Figure 5 shows the leaching yield curves for the several HCl concentrations. A test without HCl (with cupric chloride as leachant only) is also presented for comparison purposes, showing its lack of effectiveness. It is observed that the acid improves the leaching of

Pd, but this effect reduces above  $4 \text{ M}$  HCl. Concerning Rh, the yields found were substantially lower, and the leaching efficiency was not significantly improved for HCl concentrations higher than  $2 \text{ M}$ . For Rh, the temperature effect seems to be more important than the acid concentration. The same procedure described in the previous section was adopted for these series of tests, in order to estimate the  $n$  parameter that allows the best fitting. The values obtained are presented in Table 2 (first series of data for  $0.05 \text{ M Cu}^{2+}$ ) and the plots can be seen in Figure 6. For the range  $2\text{--}6 \text{ M}$  HCl the values obtained are of the same magnitude, so an average value was adopted, being  $n = 4.30$  for Pd and  $n = 5.37$  for Rh. For the lowest HCl concentration, these numbers are no longer valid, the values determined being near 3 for both metals. Figure 6 also shows that the fittings for Rh are worse than those for Pd, and for  $1 \text{ M}$  HCl the fitting for Rh is completely inadequate.

The apparent rate constants were also determined from the slopes of the fittings (Table 2) and plotted against the HCl concentration (in the log-log form), as

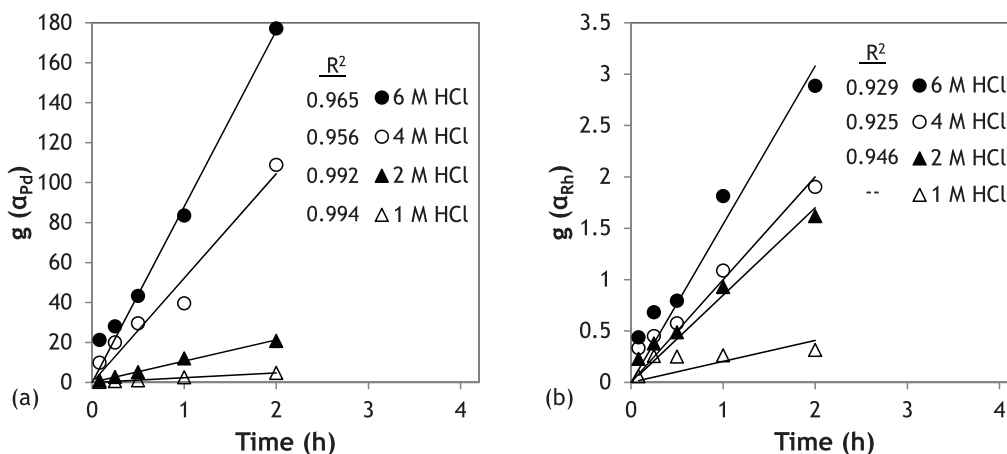


**Figure 6.** Application of the integrated rate equation to the experimental data acquired at different HCl concentrations, for (a) Pd, and (b) Rh.

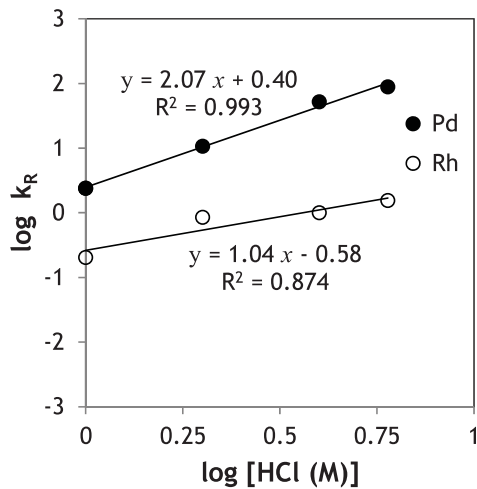


**Figure 7.** Plot of the apparent rate constants as a function of HCl concentrations for the determination of the reaction orders.

can be observed in Figure 7. This representation is based on equation (5) and allows the determination of parameter  $a$  (the reaction order referring to HCl). The values obtained were  $2.1 \pm 0.1$  for Pd and  $1.0 \pm 0.3$  for Rh. HCl concentration has thus a double power effect on the reaction rate of Pd relative to that of Rh.

A similar study was performed for the evaluation of the effect of cupric ion concentration on the reaction rates, and the subsequent determination of the respective order. The experimental data is plotted in Figure 8, showing that the presence of cupric chloride is essential to improve the rate of the reactions. When comparing the curves using different  $\text{Cu}^{2+}$  concentrations with the profile without  $\text{Cu}^{2+}$  (with HCl only) the difference for the initial period of the reactions is clear, but the dissimilarities attenuate as the reaction time is extended. The plots of  $g(a) = k_R t$  are depicted in Figure 9, and the resulting  $n$  values are also presented in Table 2 (second data series for constant 2 M HCl). In this case, all the  $n$

values determined for different concentrations were compatible, allowing the adoption of the average values (4.21 for Pd and 5.68 for Rh). The fitting for Rh at lower cupric ion concentration shows a large deviation from the linear plot, which is also observed when the predicted model is compared with the experimental data (see Figure 8(b)). For the other  $\text{Cu}^{2+}$  concentrations (0.05–0.30 M) the fittings seem to be better predictions of the reaction evolution.

In Figure 10, the log-log plot of the apparent rate constants versus  $\text{Cu}^{2+}$  concentration according to equation (5) is presented, allowing the determination of parameter  $e$  (the reaction order relative to cupric ion). The values obtained for Pd and Rh are comparable,  $0.42 \pm 0.04$  and  $0.36 \pm 0.06$ , respectively, seeming to indicate that the oxidation mechanism of both PGMs is probably similar.

### Influence of particle size and stirring

Particle size and stirring velocity are two other factors that can affect the efficiency of a leaching reaction. The particle size may influence the surface area exposed to the leachant (smaller granulometry usually leads to higher efficiency). Stirring velocity is essentially related to diffusion phenomena, since higher stirring usually promotes mass transfer of reactants and reaction products in solution, as the diffusion layer at the solid/liquid interface is reduced.

The particle size effect was evaluated by comparing the leaching behaviour of the grinded catalyst monolith with three different size distributions (standard, fine and coarse materials) prepared as described in the experimental section, and already characterized. The leaching efficiency found for Pd and Rh as a function of time, for the three granulometries, can be observed in Figure 11. The results show that the particle size has no significant effect on the leaching efficiency within the range tested.

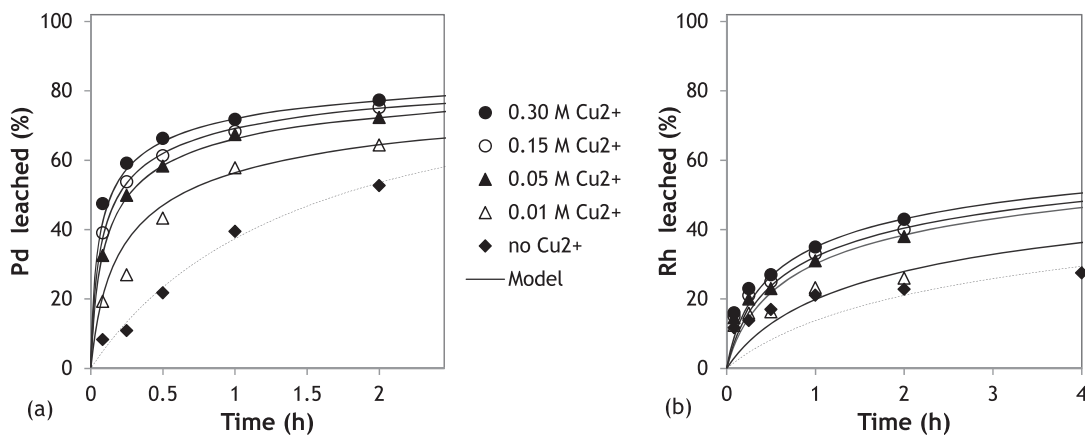


**Figure 8.** Experimental and theoretical leaching yields obtained at different  $\text{Cu}^{2+}$  concentrations, for (a) Pd, and (b) Rh ( $60^\circ\text{C}$ ;  $[\text{HCl}] = 2 \text{ M}$ ;  $R_{L/S} = 20 \text{ L kg}^{-1}$ ;  $d_{50} = 0.61 \text{ mm}$ ;  $sv = 250 \text{ min}^{-1}$ ).

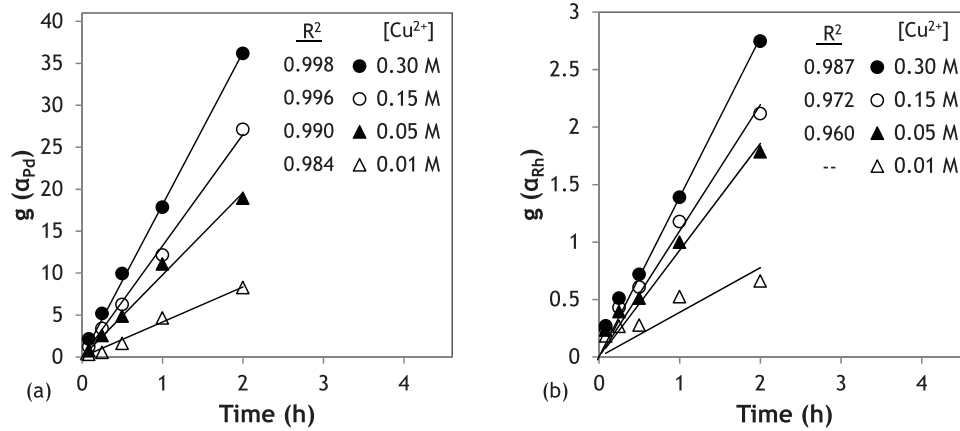


**Figure 9.** Application of the integrated rate equation to the experimental data acquired at different  $Cu^{2+}$  concentrations, for (a) Pd, and (b) Rh.

This fact is consistent with the distribution of PGMs on the surface of the monolith material (in the washcoat layer); thus, the grinding action does not seem to change the accessibility of the leachant to the PGMs. Overgrinding should be minimized for economic reasons, since this operation can only be justified to facilitate material handling or for homogenization purposes.

Concerning the stirring effect, four levels of rotational speed were tested: 80, 150, 250 and 350  $min^{-1}$ . According to the size of the paddle impeller, the correspondent tip velocities were 0.15, 0.28, 0.47 and 0.66  $m s^{-1}$ , respectively. The results obtained, depicted in Figure 12, show that stirring is not a significant parameter affecting PGMs reaction kinetics and yields. This outcome indicates that the surface chemical step is probably the most important stage of the reaction (i.e. the controlling step), the interface diffusion phenomena being less relevant. The collected data also provide values for the leaching yields

obtained at higher reaction times than the previous ones (6 h instead of 4 h). Hence, a slight increase in the leaching yields for Rh is still observed after 6 h, again corroborating that leaching is undoubtedly slower for Rh than for Pd.

### Leaching at different liquid/solid ratios

The liquid/solid ratio ( $R_{L/S}$ ) can affect the leaching efficiency in two ways: (a) the leachant amount (concentration plus volume), higher as  $R_{L/S}$  increases, determines the extent of the leaching reaction; and (b) the volume in which the metals are solubilized determines their

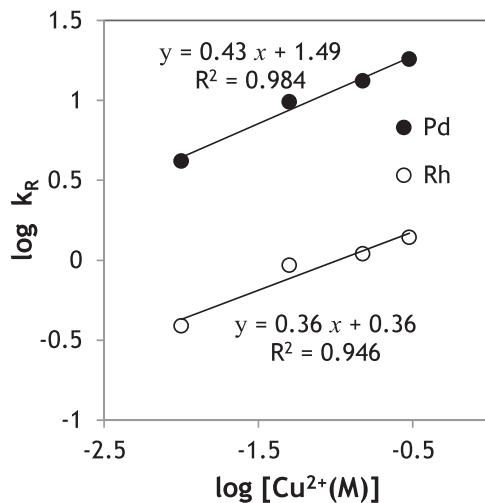


**Figure 10.** Plot of the apparent rate constants as a function of  $Cu^{2+}$  concentration for determination of the reaction orders.

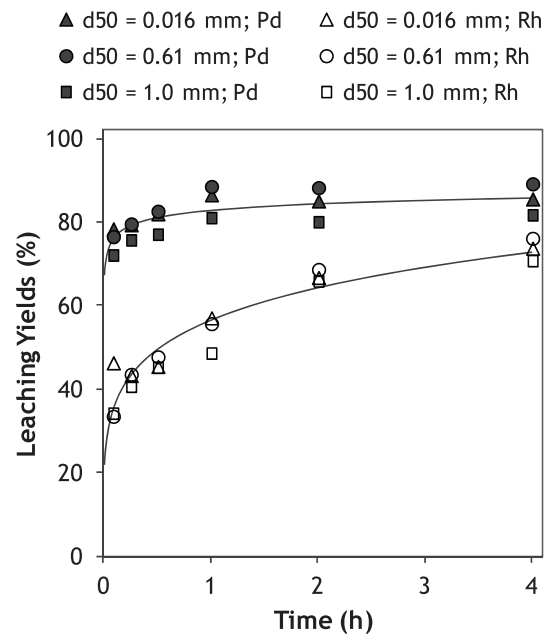


**Figure 11.** Leaching of Pd and Rh as a function of time for different particle sizes (80°C;  $[HCl] = 6 M$ ;  $[Cu^{2+}] = 0.15 M$ ;  $R_{L/S} = 20 L kg^{-1}$ ;  $sv = 250 min^{-1}$ ). Lines presented are average numerical fittings considering all the experimental points.

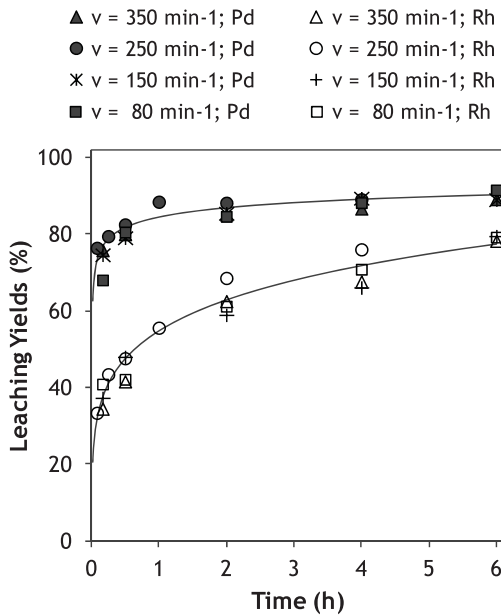


**Figure 12.** Leaching of Pd and Rh as a function of time for different stirring velocities ( $80^{\circ}\text{C}$ ;  $[\text{HCl}] = 6 \text{ M}$ ;  $[\text{Cu}^{2+}] = 0.15 \text{ M}$ ;  $R_{L/S} = 20 \text{ L kg}^{-1}$ ;  $d_{50} = 0.61 \text{ mm}$ ). Lines presented are average numerical fittings considering all the experimental points.

attainable concentrations in the leach liquor (lower as  $R_{L/S}$  increases). Optimal conditions from both technical and economical points of view are normally those corresponding to a conciliation of using values of  $R_{L/S}$  as lower as possible without compromising the reaction efficiency, in order to attain the highest possible metal concentrations in solution. Therefore, advantages can be expected in further solution processing and metals recovery efficiency, in addition to decreasing costs due to volume inventory and plant capacity.

The influence of  $R_{L/S}$  in the metals leaching was evaluated in the range of 4–20  $\text{L kg}^{-1}$  while all the other parameters remained unchanged (Figure 13). Pd and Rh

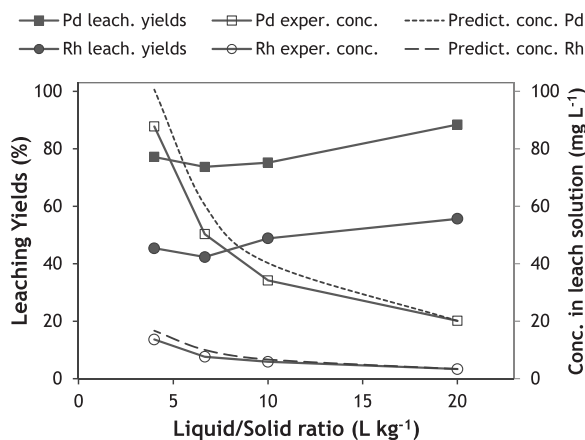


**Figure 13.** Influence of liquid/solid ratio in the Pd and Rh leaching yields, and in their correspondent concentrations in the leach solution ( $80^{\circ}\text{C}$ ;  $[\text{HCl}] = 6 \text{ M}$ ;  $[\text{Cu}^{2+}] = 0.15 \text{ M}$ ;  $t = 1 \text{ h}$ ;  $d_{50} = 0.61 \text{ mm}$ ;  $sv = 250 \text{ min}^{-1}$ ).

leaching yields are not considerably affected by this factor, although some enhancements, especially for the higher values, can be noted. Figure 13 also shows the concentrations of PGMs attained in the leach liquors. The dotted lines are the predicted Pd and Rh concentrations for the different values of  $R_{L/S}$ , determined by applying a concentration factor (inverse to  $R_{L/S}$ ) to the concentrations obtained at the higher  $R_{L/S}$  ( $20 \text{ L kg}^{-1}$ ). As an example: for Pd, the concentration observed for  $20 \text{ L kg}^{-1}$  was  $20 \text{ mg L}^{-1}$  and, therefore, a five-fold increase ( $20/4$ ) was expected in the solution concentration for  $R_{L/S} = 4 \text{ L kg}^{-1}$  for the same leaching yield. The value observed ( $88 \text{ mg L}^{-1}$ ) was lower than the one predicted ( $100 \text{ mg L}^{-1}$ ), denoting some influence of the  $R_{L/S}$ , but with a lower significance than for the other leaching factors. For Rh the observed effect was similar.

### Behaviour of other metals

The final composition of the leach liquors, namely the concentrations of the accompanying metals, is an important issue to design the best hydrometallurgical process scheme for separation, purification and recovery of PGMs. Therefore, the final leach solutions obtained in this work were analyzed for the metals identified in the catalyst monoliths. It was generally observed that, for most of them, the attained concentrations of the accompanying metals were not dependent on the conditions applied, the deviations found being normally explained by the heterogeneity of distribution. Leaching yields at room temperature and at  $100^{\circ}\text{C}$  did not vary significantly, and similar results were observed for different HCl concentrations in the presence and absence of cupric ion. The data obtained prove that it is mainly the acid that reacts with the metal species, most of them probably in the oxide forms. Significant differences with time were also not observed within the range of 1–4 h. The only remarkable variation is when the  $R_{L/S}$  was changed; for this case, the leaching yields were typically the same, but the metals concentrations increased in the inverse proportion of  $R_{L/S}$ .

Table 3 summarizes a collection of results (ranges of concentrations) that illustrate these findings. Ce, La and Zr are constituents of the washcoat of the catalyst, while the remaining metals are contaminants coming from the fuel composition, as described elsewhere [4], and emitted as fine particles in the exhaustion gases. Taking into account the initial concentrations of these metals in the catalyst, it can be concluded that the leaching efficiencies attained were relatively low for all these elements (estimated as  $<25\%$  for La and Ce, and  $<0.2\%$  for Zr). However, since Ce and La initial contents are

**Table 3.** Typical concentrations in the leach solutions, after 4 h of reaction, of other metals present in the catalyst monolith.

Test Conditions	Leach solution concentration (mg L <sup>-1</sup> )							
	Fe	Zn	Ni	Cr	Ca	Ce	La	Zr
Tests with $R_{L/S} = 20 \text{ L kg}^{-1}$ and with variation of all the other factors <sup>a</sup>	37–100	6–11	2–4	4–12	33–70	460–570	60–80	0–3
Tests with $R_{L/S} < 20 \text{ L kg}^{-1}$ <sup>b</sup>								
$R_{L/S} = 10 \text{ L kg}^{-1}$	163	13	4.5	13	33	870	126	0.9
$R_{L/S} = 6.7 \text{ L kg}^{-1}$	250	21	7	16	110	1350	194	1.5
$R_{L/S} = 4 \text{ L kg}^{-1}$	364	30	11	44	164	2270	369	2.6

<sup>a</sup>Series of tests with variation of temperature (25–100°C), [HCl] (2–6 M) and [Cu<sup>2+</sup>] (0–0.3 M).

<sup>b</sup>Tests at 80°C, 6 M HCl and 0.15 M Cu<sup>2+</sup>.

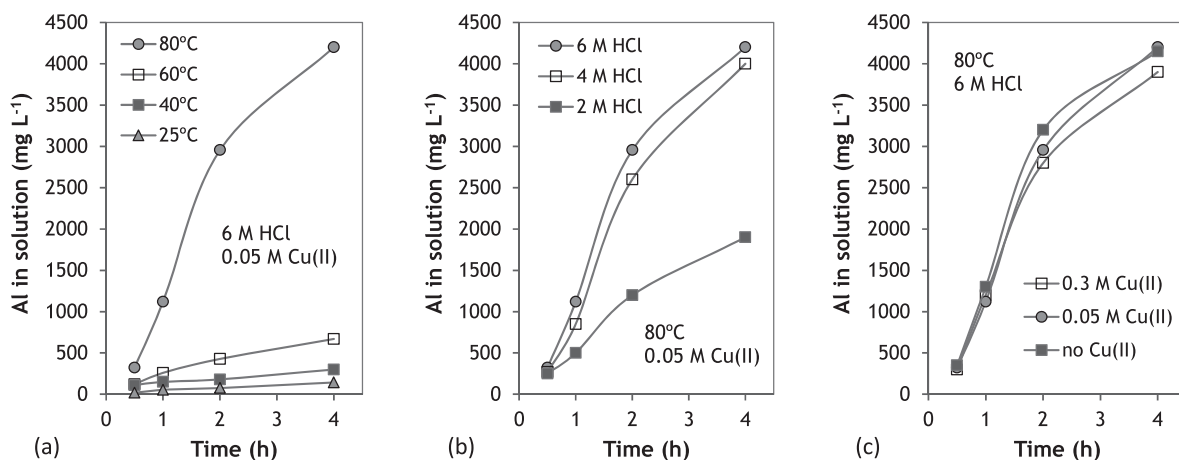


**Figure 14.** Evolution of Al dissolution in the leaching tests at different process conditions: (a) variation with temperature; (b) variation with HCl concentration; (c) variation with Cu<sup>2+</sup> concentration. Constant factors:  $R_{L/S} = 20 \text{ L kg}^{-1}$ ;  $d_{50} = 0.61 \text{ mm}$ ;  $v = 250 \text{ min}^{-1}$ .

significant, the leach solution concentrations obtained for these metals are very reasonable, particularly for Ce. These elements are valuable, and their recovery from catalysts should not be neglected. However, the recovery of Ce, La and Zr is out of the scope of the present article. Other studies have already proposed some processes for Ce recovery, namely by a previous leaching step with sulfuric acid solutions and a reducing agent [15] or by precipitation as alkali-Ce double sulfate from leach liquors [27].

Aluminum is the only exception for the behaviour previously described, since results demonstrate that its concentration in the leachates changes with the variation of the leaching factors investigated. Figure 14 shows the evolution of Al concentration with time for different values of temperature, as well as its dependence on HCl and Cu<sup>2+</sup> concentrations. In addition to the notorious effect of time, the important roles of temperature and acid concentration in Al dissolution are also well visible. Al concentrations up to near  $4 \text{ g L}^{-1}$  for the higher levels of these factors were found in the leach liquors. By the contrary, cupric ion concentrations have no effect on Al dissolution, demonstrating the acid/base character of the Al<sub>2</sub>O<sub>3</sub> leaching reaction. In the tests carried out at lower  $R_{L/S}$ , the Al concentrations obtained

increased, as values of 12 and  $14 \text{ g L}^{-1}$  Al were found for  $R_{L/S} = 6.7$  and  $4 \text{ L kg}^{-1}$ , respectively. Since the leaching conditions used in this work do not seem to promote the chemical attack of the ceramic matrix (cordierite) the only source for dissolved Al should be the Al<sub>2</sub>O<sub>3</sub> species present in the washcoat. Actually, the comparison between the initial and final weights of solids in the leaching experiments showed typical values of weight loss in the range 10%–27%, depending on the conditions. In accordance with published data [28], the washcoat material is estimated to be about 10%–25% of the total weight of a monolith, values laying within the range of weight loss observed for most of the experiments reported herein. However, two exceptions occurred, for which the weight losses were significantly higher (near 45%): the first one was for 100°C (and 6 M HCl, 0.05 M Cu<sup>2+</sup>,  $R_{L/S} = 20 \text{ L kg}^{-1}$ ) and the second for the fine ground material,  $d_{50} = 0.016 \text{ mm}$  (and 80°C, 6 M HCl, 0.15 M Cu<sup>2+</sup>,  $R_{L/S} = 20 \text{ L kg}^{-1}$ ). For these extreme conditions (of high temperature or thinner granulometry) part of the Al from the ceramic matrix should be eventually attacked and leached. In fact, this assumption is sustained by the higher Al concentrations in solution observed for the leaches coming from these two experiments (about  $9\text{--}12 \text{ g L}^{-1}$ ) when compared to the

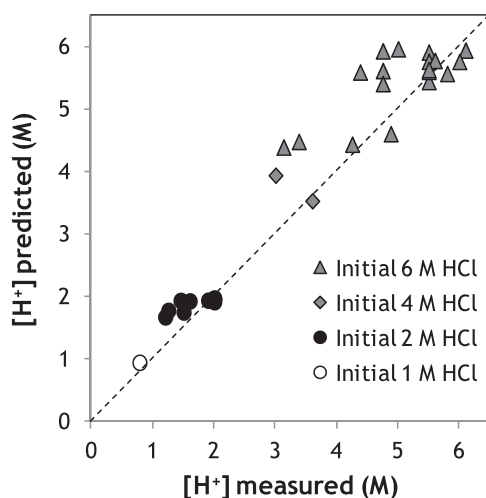


**Figure 15.** Relation between measured and predicted final  $H^+$  concentrations in leachates.

values generally obtained for all the other solutions when the same  $R_{L/S}$  was used (always  $<5 \text{ g L}^{-1}$ , with weight losses  $<27\%$ ).

The determination of the final  $H^+$  concentration in all the solutions coming from the performed leaching tests should allow the evaluation of the spent acid in the process. Figure 15 shows the relation between the measured final acidity values of the leach liquors and the ones predicted. The dotted line indicates the region where both concentrations are equal. The predicted  $H^+$  concentrations were taken from the stoichiometry of the reactions and the leaching yields achieved, considering all the analyzed metals. As an example, the contribution of dissolved Al for the predicted acid consumption was calculated from the Al concentration found in solution, and taking into account its initial form,  $Al_2O_3$ , i.e. assuming that three  $H^+$  moles are consumed per mole of Al. The experimentally measured acidity is, for some tests, lower than the predicted one, indicating that probably other reactions involving other species than those considered in this evaluation should be responsible for some acid consumption. This behaviour is more visible when higher acid concentrations are used. Nevertheless, the results demonstrate that the dissolution of  $Al_2O_3$  is the major acid consumer, accounting for near 90% or even more of the total  $H^+$  spent.

## Conclusions

The leaching of palladium and rhodium from a spent auto-catalyst in  $HCl/Cu^{2+}$  media was studied. Based on a kinetic model proposed for the present case, the influence of temperature was assessed, and the

activation energies were estimated as  $60.1 \pm 4.1 \text{ kJ mol}^{-1}$  for Pd and  $44.3 \pm 7.3 \text{ kJ mol}^{-1}$  for Rh. The chemical reaction at the catalyst surface seems to be the most relevant step, but diffusion phenomena cannot be disregarded, although being less significant. The stirring velocity was found to be irrelevant, which supports the previous conclusion. The influence of the leachant concentration was also tested, from which the reaction orders were estimated, being for HCl:  $2.1 \pm 0.1$  (Pd) and  $1.0 \pm 0.3$  (Rh); and for  $Cu^{2+}$ :  $0.42 \pm 0.04$  (Pd) and  $0.36 \pm 0.06$  (Rh). The particle size was not a relevant factor for the leaching efficiency, supporting the assumption that PGMs particles are on the surface of the catalyst, and therefore further grinding of the matrix does not significantly change the available area for the reaction to take place. The use of lower values for the liquid/solid ratio allowed the production of high Pd and Rh concentrated liquors without losing efficiency. The major contaminant of the leachates is aluminum, dissolved from the washcoat layer. To improve the selectivity for the PGMs leaching, the main process parameters, such as acid concentration, temperature and reaction time, should be adequately controlled.

## Acknowledgements

This work was supported by Portuguese national funds through FCT – Fundação para a Ciência e a Tecnologia (Lisbon, Portugal), under the projects reference numbers PTDC/QUI-QUI/109970/2009, UID/Multi/04326/2019 and UID/MULTI/00612/2013. In the leaching experimental procedures the collaboration of the technician Natália Oliveira from LNEG is also acknowledged.

## Disclosure statement

No potential conflict of interest was reported by the authors.

## Funding

This work was supported by Portuguese national funds through FCT – Fundação para a Ciência e a Tecnologia (Lisbon, Portugal), under the projects reference numbers PTDC/QUI-QUI/109970/2009, UID/Multi/04326/2019 and UID/MULTI/00612/2013.

## References

- [1] Heck RM, Farrauto RJ. Automobile exhaust catalysts. *Appl Catal A-Gen.* 2001;221:443–457.
- [2] Erdmann L, Graedel TE. Criticality of non-fuel minerals: a review of major approaches and analyses. *Environ Sci Technol.* 2011;45:7620–7630.
- [3] Hagelüken C. Recycling the platinum group metals: a European perspective. *Platinum Metals Rev.* 2012;56:29–35.

- [4] Hagelüken C. Precious metals process catalysts – materials flows and recycling. *Chem Today (Supplement)*. 2006;24:14–17.
- [5] Crundwell FK, Moats MS, Ramachandran V, et al. Extractive metallurgy of nickel, cobalt and platinum-group metals. Amsterdam: Elsevier; 2011.
- [6] Jha MK, Lee JC, Kim MS, et al. Hydrometallurgical recovery/recycling of platinum by the leaching of spent catalysts: a review. *Hydrometallurgy*. 2013;133:23–32.
- [7] Dong H, Zhao J, Chen J, et al. Recovery of platinum group metals from spent catalysts: a review. *Int J Miner Process*. 2015;145:108–113.
- [8] Jimenez de Aberasturi D, Pinedo R, Ruiz de Larramendi I, et al. Recovery by hydrometallurgical extraction of the platinum-group metals from car catalytic converters. *Miner Eng*. 2011;24:505–513.
- [9] Harjanto S, Cao Y, Shibayama A, et al. Leaching of Pt, Pd and Rh from automotive catalyst residue in various chloride based solutions. *Mater Trans*. 2006;47:129–135.
- [10] Cao Y, Harjanto S, Shibayama A, et al. Kinetic study on the leaching of Pt, Pd and Rh from automotive catalyst residue by using chloride solutions. *Mater Trans*. 2006;47:2015–2024.
- [11] Fornalczyk A, Saternus M. Catalytic converters as a source of platinum. *Metalurgija*. 2011;50:261–264.
- [12] Barakat MA, Mahmoud MHH. Recovery of platinum from spent catalyst. *Hydrometallurgy*. 2004;72:179–184.
- [13] Potgieter JH, Potgieter SS, Mbaya RKK, et al. Small-scale recovery of noble metals from jewellery wastes. *J S Afr I Min Metall*. 2004;104:563–572.
- [14] Angelidis TN, Skouraki E. Preliminary studies of platinum dissolution from a spent industrial catalyst. *Appl Catal A-Gen*. 1996;142:387–395.
- [15] Angelidis TN. Development of a laboratory scale hydro-metallurgical procedure for the recovery of Pt and Rh from spent automotive catalysts. *Top Catal*. 2001;16/17:419–423.
- [16] Chen S, Shen S, Cheng Y, et al. Effect of O<sub>2</sub>, H<sub>2</sub> and CO pre-treatments on leaching Rh from spent auto-catalysts with acidic sodium chlorate solution. *Hydrometallurgy*. 2014;144–145:69–76.
- [17] Chen A, Wang S, Zhang L, et al. Optimization of the microwave roasting extraction of palladium and rhodium from spent automobile catalysts using response surface analysis. *Int J Miner Process*. 2015;143:18–24.
- [18] Kasuya R, Miki T, Morikawa H, et al. Dissolution of platinum in catalyst materials using hydrochloric acid: a new method based on the use of complex oxides. *Miner Eng*. 2016;87:25–31.
- [19] Suoranta T, Zugazua O, Niemelä M, et al. Recovery of palladium, platinum, rhodium and ruthenium from catalyst materials using microwave-assisted leaching and cloud point extraction. *Hydrometallurgy*. 2015;154:56–62.
- [20] Steinlechner S, Antrekowitsch J. Potential of a hydrometallurgical recycling process for catalysts to cover the demand for critical metals like PGMs and cerium. *JOM – J Miner Met Mat Soc*. 2015;67:406–411.
- [21] Nogueira CA, Paiva AP, Oliveira PC, et al. Oxidative leaching process with cupric ion in hydrochloric acid media for recovery of Pd and Rh from spent catalytic converters. *J Hazard Mater*. 2014;278:82–90.
- [22] Habashi F. Principles of extractive metallurgy – general principles. New York: Gordon and Breach Science Publishers Ltd; 1980.
- [23] Havlik T. Hydrometallurgy – principles and applications. Cambridge: CISP, Florida: CRC Press; 2008.
- [24] Levenspiel O. Chemical reaction engineering. New York: John Wiley & Sons; 1999.
- [25] Kim W, Kim B, Choi D, et al. Selective recovery of catalyst layer from supporting matrix of ceramic-honeycomb-type automobile catalyst. *J Hazard Mat*. 2010;183:29–34.
- [26] Baghalha M, Khosravian H, Mortaheb HR. Kinetics of platinum extraction from spent reforming catalysts in aqua-regia solutions. *Hydrometallurgy*. 2009;95:247–253.
- [27] Rumpold R, Antrekowitsch J. Recycling of platinum group metals from automotive catalysts by an acidic leaching process, Platinum'2012 - Fifth International Platinum Conference 'A catalyst for change'; 2012 Sep 17–21; Sun City. Johannesburg: The Southern African Institute of Mining and Metallurgy; 2012. p. 695–714.
- [28] Kim CH, Woo SI, Jeon SH. Recovery of platinum-group metals from recycled automotive catalytic converters by carbochlorination. *Ind Eng Chem Res*. 2000;39:1185–1192.